A Comparative Study Of Linear And Non-Linear Methods of Isotherm Parameters For Biosorption Of Sodium Diclofenac Onto Calcined Cow Leather (CCL)

Hasnaa Hiyane
Hassan II University
Saida Benkaddour
Hassan II University
R. Slimani
Hassan II university
Benoît Cagnon
University of Orleans
Khalid Karrouchi
National laboratory of Drugs control, Rabat
Mohammadine EL Haddad
Cadi Ayyad University
Youness Achour
Sultan Moulay Slimane University https://orcid.org/0000-0001-8183-0898
Said EL Antri
Hassan II university
Said Lazar (lazar_said@yahoo.fr)
University Hassan II Casablanca

Research

Keywords: UV-Visible spectroscopy, Sodium diclofenac, Natural adsorbent, Adsorption, linear and non-linear isotherm, anti-inflammatory

Posted Date: May 6th, 2021

DOI: https://doi.org/10.21203/rs.3.rs-465341/v1

A comparative study of linear and non-linear methods of isotherm parameters for biosorption of Sodium Diclofenac onto Calcined Cow Leather (CCL)

H. HIYANE[1], S. BENKADDOUR[1], R. SLIMANI[1], B. CAGNON[2], K. KARROUCHI[3], M. EL HADDAD[4], Y.ACHOUR[4,5], S. EL ANTRI[1], S. LAZAR[1*]

[1]Laboratory of Biochemistry, Environment & Food, UARC 36, University Hassan II Casablanca, Mohammedia, Morocco.
[2]Interfaces, Containment, Materials & Nanostructures (ICMN-UMR 7374). CNRS - University of Orleans, France.
[3]National Laboratory of drugs control, Rabat, Morocco.
[4]Laboratory of analytical and molecular chemistry, Faculté Poly-disciplinaire, University of Cadi Ayyad, BP 4162, 46000 Safi, Morocco.
[5]Laboratory of Organic and Analytical Chemistry, Faculty of Science and Technology, Sultan Moulay Slimane University, BP 523, 23000 Beni-Mellal, Morocco

*Corresponding author at: BP 146, 20650 Mohammedia, Morocco.
E-mail address: SAID.LAZAR@univh2c.ma / lazar_said @yahoo.fr (S. Lazar)
Tel : +212 5 23 31 47 05 / Fax : +212 5 23 31 53 53

Abstract

In the current work, the activated biosorbent prepared from Calcined Cow Leather (CCL) was used to study the biosorption potential on anti-inflammatory, namely Sodium Diclofenac and derived from phenylacetic acid from the group of arylcarboxylic acids. Thus, it has been selected because they are widely used and potential associated toxicological effects and also apparently detected in aqueous environments. The biosorption study was carried out to examine the biosorption mechanism by applying the five isotherms models represented by the Langmuir, Freundlich, Elovich, Temkin and Dubinin-Radushkevich. The comparison of linear and nonlinear regression methods was applied by taking into consideration mathematical and statistical properties of these two methods and compare different statistical criteria to determine the best model fitted to experimental data by predicting the optimum isotherms parameters. The following six error functions were used, the coefficient of determination (R^2), the sum of

the squares of the errors (SSE) , Hybrid fractional error function (HYBRID), Average relative error (ARE) , Sum of the absolute errors (SAE) and Marquardt's percent standard deviation (MPSD). Whereas, the comparison between different models shows that the nonlinear form of Langmuir model was the best fitted to describe the equilibrium data which was confirmed by the five error functions and the smallest 'sum of the normalized errors (SNE)' parameter. Therefore, the kinetics data was evaluated by various models. It was found that the biosorption process was conducted by the pseudo-second-order model which predicted best the experimental data.

Keywords: *UV-Visible spectroscopy, Sodium diclofenac, Natural adsorbent, Adsorption, linear and non-linear isotherm, anti-inflammatory.*

1. Introduction

Water is a vital resource for all living creatures. Unfortunately, It is threatened by pollution that is becoming increasingly important, linked to the release of dangerous chemical compounds by different industries: chemicals, textiles, tanneries, agribusiness, pharmaceuticals … etc.

Among these pollutants, many molecules come from pharmaceutical industries. Medicated residues, rejected by industries, but also by hospitals, industrial farms (large consumers of antibiotics) or domestic urine and stool. These residues are detected today at very low concentrations ($ng.L^{-1}$ or $\mu g.L^{-1}$) in aquatic environment thanks to analytical devices performing. The revelation of the omnipresence of pharmaceutical chemicals (ketoprofen, naproxen, ketotifen and diclofenac…) into the environment has given rise to a new concern, due to their intrinsic biological activity, photodegradation sensitivity and inherent toxicological effects **[1].** In addition, Sodium Diclofenac (SD) contains several structural motifs, which are photochemically active and also reactive toward photochemically generated oxidizing agents, such as the hydroxyl radical and singlet oxygen.

Many water treatment techniques have been developed in recent years. These techniques include chemical precipitation processes, flocculation, ion exchange, electrolysis, membrane processes; however present dissatisfactory results because of the formation of residual toxic by-products in addition to high treatment cost. Hence, many researchers shifted their interest to adsorption technique due to their efficiency and cheaper cost and also the low cost of biosorbents prepared form vegetal wastes using *Cyclamen persicum* **[2],** cocoa pod husks **[3],** olive stones **[4],** Tea waste **[5]**, cocoa shell **[6]** and potato peel waste **[7]** or from animal wastes, such as chicken feathers **[8],** animal bones **[9],** *Ensis siliqua* Shells **[10]** and snail shells **[11].** In the current work, the used biosorbent is the Calcined Cow Leather (CCL) which presents an abundant slaughterhouse waste especially at Eid al-Adha holiday. Thus, the CCL biosorbent was used to study the adsorption potential of pharmaceutical products. On the other hand, as to describe well the equilibrium adsorption, the linear and nonlinear forms of two-parameter isotherm models are frequently conducted to give the right description and characterization to adsorption mechanism. However, the primary aim of this work is to shed more light on the comparison of these two methods by taking into consideration mathematical and statistical properties of these two methods and compare different statistical criteria to determine the best model fitted to experimental data and isotherm parameters.

2. Materials and methods

2.1.Material

Cow leathers used in this work were collected previously from a slaughterhouse's management waste service located in Casablanca city (Morocco), cleaned from blood and other dirt, and salted immediately with common marine salt. Dried in open air for many days for partial removal of water. Then, dried at 70 °C until reach a constant weight. Dried leathers were calcined for 4 hours at 525 °C. The residue ground to fine powder, passed through sieves and particles were collected under 200 µm and rinsed with deionized water until reached pH = 7,

then dried for 24 hours at 105 °C. The residual material was kept in a plastic container and preserved in a desiccator for further use and the Calcined Cow Leathers were abbreviated (CCL).

2.2.Preparation of Sodium Diclofenac (SD) standards

The synthetic stock solution (1 $g.L^{-1}$) used in these studies was prepared by dissolving 100 mg of powdered sodium diclofenac (SD) (99% purity) in 100 mL deionized water. All desired test solutions (0.0-60mg/L) were prepared from appropriate dilution of stock solution. The calibration curve was depicted at this point, by plotting absorbance values vs. Initial concentrations of SD standard solutions to verify Beer-Lambert's law (Figure 1), in order to determine the areas of concentrations. The physic-chemical properties and chemical structure of SD drug are shown in Table 1.

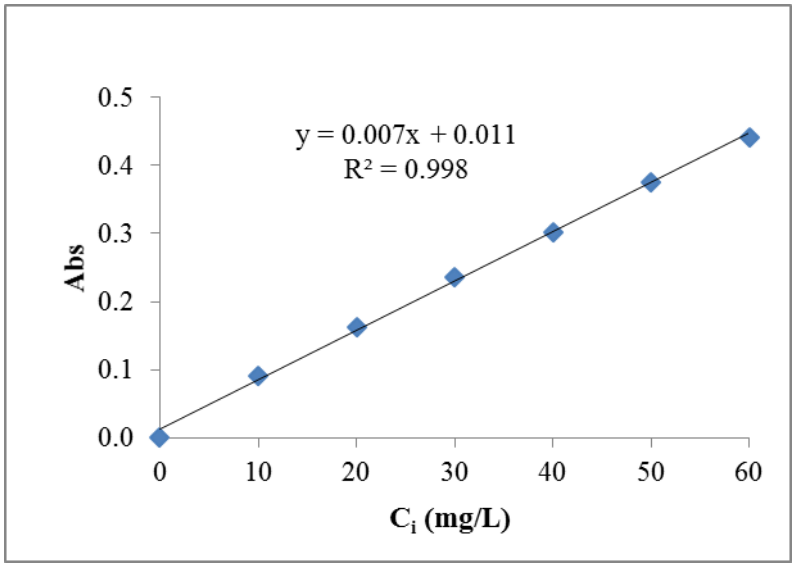

Figure 1: Calibration curve of SD.

Table 1: Physicochemical properties and chemical structure of Sodium Diclofenac.

	Sodium Diclofenac[12]
Chemical formula	$C_{14}H_{10}Cl_2NNaO_2$
Systematic name	sodium 2-{2-[(2,6-dichlorophenyl)amino] phenyl} acetate

Chemical structure	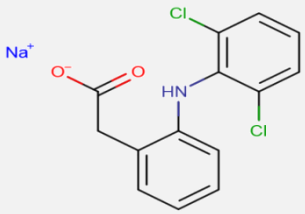
Molecular weight	318.1 g/mol
Use	Nonsteroidal anti-inflammatory drug and as an analgesic
Solubility in water (mg/L, 25°C)	0.00482 mg/mL
Log K_{ow} (at pH= 7)	1.37
pK_a (25°C)	4.2
λ_{max}	310 nm
Purity	99%

98

99 **2.3.Physical and chemical CCL characterization**

100 The biosorption efficiency of the activated biosorbent (CCL) is highly influenced by the
101 physical and chemical properties, for this purpose the prepared biosorbent (CCL) was
102 characterized for its physical characteristics by the BET method using a pore size micromeritics
103 ASAP 2020 apparatus (USA) to determine the specific surface area (BET). SEM analysis (FEI
104 Quanta 200 instrument (USA)) was performed to study the surface morphology of the
105 biosorbent (CCL). Furthermore, the chemical properties of the prepared biosorbent were
106 determined in terms of elemental composition analysis by Energy Dispersive X-rays
107 Spectroscopy (EDXS): X'Pert Pro MPD Panalytical (Netherlands) with Cu anode as the source
108 of X-rays at wavelength λ=1.54 Å including ultimate (C, H, N and others) and XRF analysis
109 for CCL and also Fourier Transform Infrared Spectroscopy (FTIR) analysis was carried out in
110 the 450-4000cm^{-1} to determine the molecular structure of the functional groups and the
111 chemical bonds that exist on the sample of the prepared biosorbent under investigation using
112 an FT/IR-Vertex 70 spectrometer (Germany).

113

2.4.Adsorption procedure

The biosorption experiments were performed in batch system to study the effectiveness of SD removal by taking into consideration the effects of the following parameters: biosorbent dosage (0.05-0.2 g), initial concentration (10- 60 mg/L), contact time (15- 240min), temperature (25, 35, 45 and 55°C), and pH (2- 10). Biosorption kinetics, isotherms and thermodynamic are also studied in this work. For pH Adjustment, Hydrochloric acid (HCl, 37%, Sigma Aldrich) and sodium hydroxide solutions (NaOH, 36–38%, Merck) were used and measured using the pH-Meter (METROHM 691). These samples were shaken with a magnetic stirrer (IKA, RT 10 power) at 400 rpm with appropriate time and temperature then filtrated using Fioroni filter paper, as final step the residual supernatants were analyzed using UV-Visible spectrophotometer for all spectral measurements at 310 nm, Nitric acid 69–71% was used with assay for SD **[13]** and all samples were performed in duplicate. The removal percentage of SD from its solution was calculated as:

$$\%\boldsymbol{R} = \frac{\boldsymbol{C_i - C_f}}{\boldsymbol{C_i}} \times \mathbf{100} \qquad \text{(Eq.1)}$$

Where C_i is the initial concentration of SD (mg/L) and C_f is the final concentration (mg/L).

The metal uptake q (mg/g) was estimated following the equation **[14]:**

$$\boldsymbol{q_e} = \frac{\boldsymbol{C_i - C_f}}{\boldsymbol{m}} \times \boldsymbol{V} \qquad \text{(Eq.2)}$$

Where m is the quantity of biosorbent (g) and V is the volume of the suspension (L).

2.5.Isotherm Modeling

Many mathematical isotherm models have been developed. The most widely used are the Langmuir and Freundlich models because their mathematical expression is simple, and they make it possible to correctly represent the isothermal equilibrium adsorption in the aqueous phase in the majority of cases. Other models are more complex, but they have been developed more recently to describe the adsorbent-adsorbate interactions. Finally, those models are allowing us to predict the simultaneous adsorption of several compounds. The biosorption mechanism of CCL biosorbent on the active substance of Sodium Diclofenac (SD) in the present study was modeled by the Langmuir, Freundlich, Elovich, Temkin and Dubinin-Radushkevich (two-parameter) isotherm equations (Table 2).

Table 2: Two-parameter models studied in this study.

Isotherms	Noninear form	Linear form	Plot
Langmuir **[15]**	$\frac{q_e}{q_m} = \frac{K_L C_e}{1 + K_L C_e}$	$\frac{1}{q_e} = \frac{1}{C_e}\frac{1}{q_m K_L} + \frac{1}{q_m}$	$\frac{1}{q_e}$ vs $\frac{1}{C_e}$
Freundlich **[16,17]**	$q_e = K C_e^{1/n}$	$\log(q_e)=\log(K_F)+(1/n)\log(C_e)$	$\log(q_e)$ vs. $\log(C_e)$
Temkin **[18]**	$\frac{q_e}{q_m} = \frac{RT}{\Delta Q}\ln(K_T C_e)$	$q_e=B_T \ln K_T + B_T \ln C_e$ (with $B_T = \frac{q_m RT}{\Delta Q}$)	$q_e$vs. $\ln C_e$
Elovich **[19]**	$\frac{q_e}{q_m} = K_E C_e \exp(q_e/q_m)$	$\ln\left(\frac{q_e}{q_m}\right) = \ln(K_E C_e) + \frac{q_e}{q_m}$	$\ln\left(\frac{q_e}{q_m}\right) vs q_e$
Dubinin–Radushkevich **[20]**	$q_e = q_m \exp(-\beta\varepsilon^2)$ (with $\varepsilon = RT\ln(1+\frac{1}{q_e})$)	$\ln(q_e)=\ln(q_m) - \beta\varepsilon^2$	$\ln(q_e)$ vs ε^2

2.6.Biosorption kinetics

The biosorption kinetics provides the rate of biosorbate uptake onto the activated biosorbent within the equilibrium contact time. In this study, two models were implemented to evaluate

the rate constant of the biosorption process: The pseudo-first-order and pseudo-second-order kinetic models gathered in Table 3.

Table 3: Lagergren Kinetic models pseudo-first -order and pseudo-second-order forms

Kinetic model	Linear form	Plot
Pseudo-first-order **[21]**	$Ln(q_t - q_e) = ln(q_e) - k_1.t$	$Ln(q_t - q_e)$ vs. t
Pseudo-second-order **[22]**	$t/q_t = 1/K_2q_2 + t/q_e$	t/q_t vs. t

2.7.Error analysis

Recently, linear regression has been one of the most viable tools defining the best fitting relationship quantifying the distribution of adsorbate, mathematically analyzing the adsorption systems. Non-linear optimization provides method for determining isotherm parameter values but still requires an error function assessment, in order to evaluate the fit of the isotherm to the experimental results. Since the choice of error function can affect the parameters derived. In this study six non-linear error functions (sum squares errors, hybrid fractional error function, Marquardt's percent standard deviation, average relative error, sum of absolute error and the coefficient of determination) (Table 4) were examined to evaluate the accuracy of each model isotherm equation to the experimental data (Table 2).The interpretation method chosen based on the simple plot ("Excel" software) allowing the linearization and evaluation of the parameters values for each model. Secondly, an interpretation using nonlinear regression algorithms using Satatistica version 10 software was tested to study nonlinear forms. Contrary to the linearization models, nonlinear regression usually involves the minimization or maximization of error distribution (between the experimental data and the predicted isotherm) based on its convergence criteria **[23].**

Table 4: List of error functions [**24-28].**

Error Function	**Abbreviation**	**Definition**

Sum of quadratic gaps	ERRSQ / SSE	$\sum_{i=1}^{n}(q_{e,calc}-q_{e,mes})_i^2$
Hybrid fractional error function	HYBRID	$\frac{100}{n-p}\sum_{i=1}^{n}\left[\frac{(q_{e,meas}-q_{e,calc})}{q_{e,meas}}\right]_i$
Marquardt's percent standard deviation	MPSD	$100\sqrt{\frac{1}{n-p}\sum_{i=1}^{n}\left(\frac{(q_{e,meas}-q_{e,calc})}{q_{e,meas}}\right)_i^2}$
Average relative error	ARE	$\frac{100}{n}\sum_{i=1}^{n}\left\|\frac{(q_{e,meas}-q_{e,calc})}{q_{e,meas}}\right\|_i$
Sum of the absolute errors	SAE	$\sum_{i=n}^{n}\left\|q_{e,calc}-q_{e,meas}\right\|_i$
The Coeffcient of determination	R^2	$\frac{(q_{exp}-\overline{q_{cal}})^2}{\sum(q_{exp}-\overline{q_{cal}})+(q_{exp}-q_{cal})^2}$

3. Results and discussion

In this study, five error functions were examined for isotherm equations and in each case a set of isotherm parameters were determined by minimizing seven well-known error functions to calculate the error deviation between experimental and predicted equilibrium adsorption data of linear and nonlinear methods on the concentration range studied. The error functions studied are mentioned previously on the precedent section. As known, each error function produces a different set of isotherm parameters, due to the difficulty of a direct identification towards the total optimal parameters. However, the parameter "SNE" is used in order to have a better comparison between the sets of parameters for the same isothermal model **[29-31].**

The calculation method for the 'sum of the normalized errors' (SNE) is as follows:

(a) Select one isotherm and one error function and determine the isotherm parameters that minimize the error function for that isotherm to produce the isotherm parameter set for that error function.

(b) Determine the values for all the other error functions for that isotherm parameter set.

(c) Calculate all other parameter sets and all their associated error function values for that isotherm.

(d) Select each error measure in turn and ratio the value of that error measure for a given parameter set to the largest value of that error from all the parameter sets for that isotherm.

(e) Sum all these normalized errors for each parameter set.

The smallest sum normalized error (SNE) is considered to be optimal for that isotherm provided. Modeling of equilibrium isotherms according to the linear and non-linear models of Langmuir, Freundlich, Temkin, Elovich and D-R was performed and the values of the five error functions of the two-parameter isotherms investigated in this study are listed in Tables 5 and 6. Based on the R^2 coefficient values, the analysis of non-linear model of Langmuir is the best fitted for SD using experimental data, since this model has the highest correlation coefficient, the lowest values of errors functions and SNE value as well. The analysis of the error function results confirms the model determined based on the R^2 correlation coefficient values for the nonlinear regression, but disagrees with the model determined by the linear regression, which confirms by comparing and studying all the resulted values of error functions and taking into consideration the inherent distortion resulting from the linearization of non-linear forms, that the parameters of the non-linear form cannot be solved from the linear equation, so the nonlinear regression is more precise, efficient and gives exact results than linear regression for the modeling of the adsorption isotherms. The highest R^2 and the lowest SSE, HYBRID, MPSD, ARE, SAE and SNE are in bold.

Table 5: The linear and nonlinear isotherm models constants for SD biosorption onto CCL biosorbent.

Diclofenac	**Langmuir**

Linear form	K_L =0.152L/mg	q_m = 18.140mg/g	R_L =0.397
Nonlinear form	K_L=0.150L/mg	q_m=18.678mg/g	R_L = 0.401
	Freundlich		
Linear form	K_F =2.270 $mg^{(1-n)}$ Ln g^{-1}		n= 1.192
Nonlinear form	K_F = 2.495$mg^{(1-n)}$ Ln g^{-1}		n=1.346
	Temkin		
Linear form	K_T = 2.135L/mg		B_T = 3.203
Nonlinear form	K_T =2.146L/mg		B_T =1.388
	Elovich		
Linear form	K_E =0.135 L/mg		q_m = 19.231mg/g
Nonlinear form	K_E = 0.150L/mg		q_m=13.194mg/g
	Dubinin–Radushkevich		
Linear form	q_m = 6.573mg/g	β =1.10^{-6}	E=707.11 kJ/mol
Nonlinear form	q_m = 8.373mg/g	β = 2.10^{-6}	E=500.501kJ/mol

Table 6: Error functions values of the two-parameter isotherm models for the linear and nonlinear forms of diclofenac (SD) biosorption on CCL

	Model form	R^2	SSE	HYBRID	ARE	SAE	MPSD	SNE
Langmuir	Nonlinear	**0.998**	0.085	1.505	2.478	0.511	9.460	**0.280**
	Linear	0.773	17.620	154.620	28.899	9.333	75.571	5.000
Freundlich	Nonlinear	0.994	0.250	3.913	7.379	0.963	14.940	0.596
	Linear	0.990	0.552	3.839	7.210	1.415	10.375	0.595
Temkin	Nonlinear	0.996	0.203	1.864	5.582	0.964	8.762	0.436
	Linear	0.996	0.193	1.749	5.369	0.934	8.451	0.420
Elovich	Nonlinear	0.997	0.151	2.611	5.800	0.676	12.413	1.064
	Linear	0.993	0.376	2.823	6.517	1.238	9.345	0.521
R-D	Nonlinear	0.932	3.202	25.142	19.880	3.825	27.367	1.804
	Linear	0.881	3.964	24.631	15.702	3.648	23.484	1.629

Biosorption kinetics

Figures 2 illustrates the plot of ln(qe-qt) versus time (t) for the pseudo-first-order of SD on CCL at different concentrations. The values of $K_{ads,1}$ can be predicted and $q_{e,cal}$ can be also determined from the intercept and the slope when t=0. However, Figure 3 shows the plot of t/qt against t (minutes) which gives $1/qe_{(cal)}$ as the slope and $1/k_2q^2_e$ as the intercept, where k_2 ($g.mg^{-1}.min^{-1}$) is the rate constant of the second-order biosorption.

Figure 2 shows the nonlinearity of the plot of ln(qe-qt) as a function of time (t). This indicates that the biosorption kinetics of diclofenac is not controlled by the first model. Whereas, Figure 3 indicates that physical adsorption plays an important role in SD adsorption onto CCL. Overall, the pseudo-second-order kinetic model fits the experimental data better than the pseudo-first-order kinetic model as it correlates the experimental data well for all concentrations for the selected active substance (SD) under investigation.

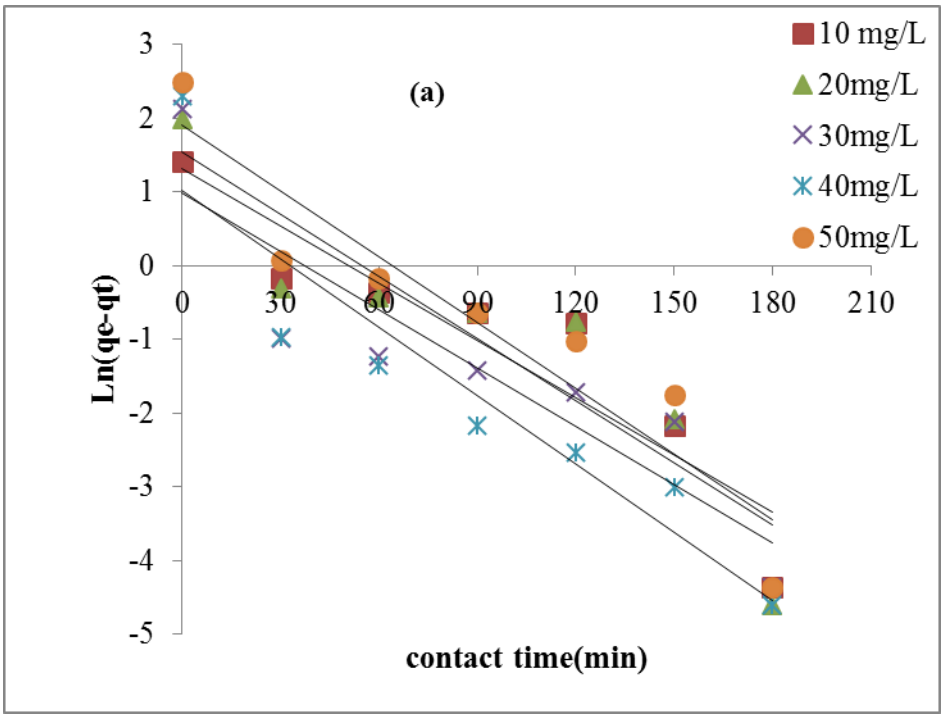

Figure 2: Linearized plots for Pseudo-first-order kinetics for biosorption of sodium diclofenac (SD) onto CCL biosorbent.

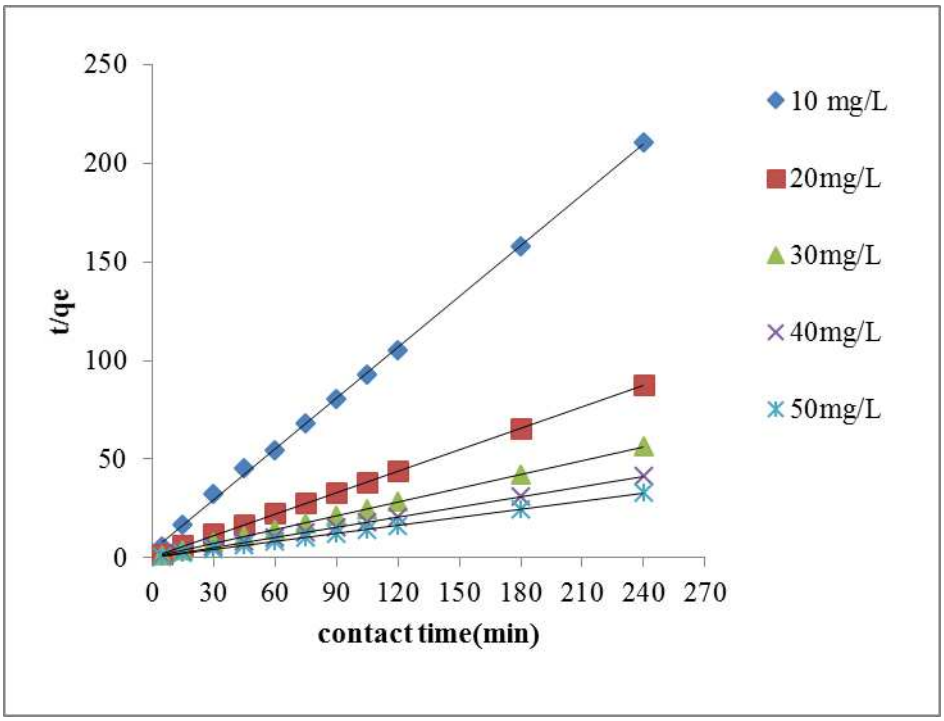

Figure 3: Linearized plots for Pseudo-second-order kinetics for biosorption of sodium diclofenac (SD) onto CCL biosorbent.

It is observed that the regression lines are almost superimposed by the experimental data. All of the kinetic parameters determined from these figures are expressed in Table 7, which indicate that the values of the correlation coefficient (R^2) for the linear model of the pseudo-first-order are far from unity. The values of $q_{e,exp}$ are incomparable with those of $q_{e,cal}$, which confirm that the system is not well fitted to the pseudo-first-order equation which is inadequate to obtain good adsorption kinetics. Accordingly, the pseudo-second-order equation was applied. Therefore, all the R^2 values obtained from the pseudo-second-order model are closer to unity, indicating that the biosorption of SD on the activated biosorbent studied fits the model well. Moreover, the experimental $q_{e,exp}$(mg/g) values agreed satisfactorily with the calculated values $q_{e,cal}$(mg/g). The pseudo-second-order kinetic model is based on the assumption that chemical adsorption is the rate controlling step. It can predict the behavior over the whole range of contact period **[32-34].** This suggests that the overall rate of the adsorption process studied

here is controlled by chemisorption which proceeds by the exchange or sharing of valance electrons between the biosorbate and biosorbent.

Table 7: Lagergren pseudo-first-order and pseudo-second-order kinetics biosorption parameters for SD biosorption onto CCL at 25 ℃.

		Pseudo-First order				Pseudo-Second order		
	C_e (mg/L)	$q_{e,exp}$ (mg/g)	$q_{e,cal}$ (mg/g)	$K_{ads,1}$ (min^{-1})	R^2	$q_{e,cal}$ (mg/g)	$K_{ads,2}$ (min^{-1})	R^2
Diclofenac	10mg/L	1.143	0.311	0.019	0.792	1.168	0.188	0.999
	20mg/L	2.738	0.475	0.020	0.742	2.770	0.184	0.999
	30mg/L	4.238	0.516	0.022	0.717	4.292	0.142	0.999
	40mg/L	5.786	0.807	0.022	0.784	5.848	0.102	0.999
	50mg/L	7.310	0.855	0.025	0.841	7.407	0.077	0.999

Physical and chemical characterization

The chemical composition is determined by X-ray fluorescence. The elemental analysis of CCL shows an abundant presence of oxygen (65.5%) and carbon (21.5%) followed up by small amounts of other elements such as calcium (2.71%), sodium (2.59%), phosphorus (2.01), chlorine (1.71), magnesium (1.32%), silicon (1.08%), sulfur (0.728%), aluminum (0.302%), iron (0.252%), potassium (0.142%), zinc (0.029%), strontium (0.019%), titanium (0.015%), iodine (0.009%), bromine (0.005%) and copper (0.004%).

The activated carbon (CCL) was submitted to IR spectroscopy as depicted in figure 4. The two closest and acute bands around 2800-2900cm^{-1} appear in the spectrum correspond to asymmetric and symmetric C-H stretching vibrations of aliphatic groups, -CH_3 and –CH_2. The closest peaks at 2300-2400 cm^{-1} are found on the spectrum of the activated carbon prepared

from calcined cow leather which shows the presence of carboxylic acid, -COOH functional group. The overlapped bands at the 1500-1650 cm^{-1} region are due to C=C stretching vibrations in sp^2 hybridized carbons in polyaromatics rings. The strong band at 1000-1150 cm^{-1} region is a very typical absorption for activated carbons in general and has been ascribed to either a C-O stretching vibration or to a Si-O stretching vibration mineral matter contained in the carbon (silicates), which may be due to inorganic silicates in the calcined cow leather sample. The peaks detected at 1000-1100 cm^{-1} in the spectrum of the CCL biosorbent reveals the presence of C-O-C stretching vibrations of esters, ether or phenol groups whereas the weak to medium peaks located at 500-800 cm^{-1} are assigned for C-H out-of plane bending of benzene derivatives, O-H stretching vibrations of C-O-H band. The results obtained agreed with the previous research where C-H out-of plane bending vibration for benzene derivatives were found on the surface of various activated carbons **[35]**, whereas O-H functional group has been found on the surface of most of the activated carbons, including the commercial grade activated carbons **[36]**.

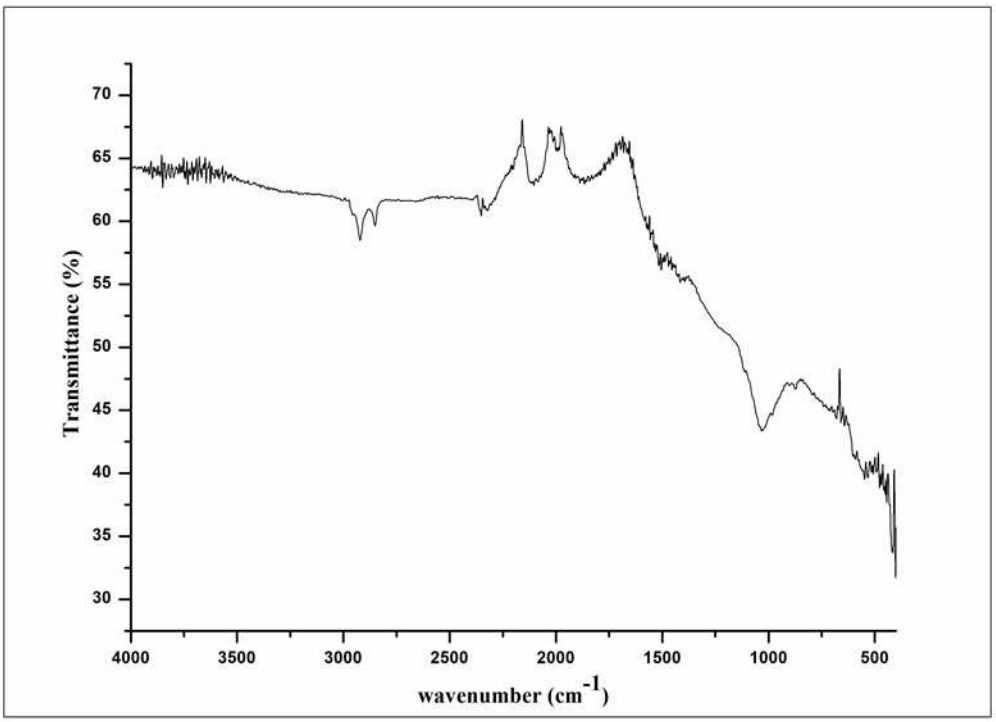

Figure 4: IR spectrum of biosorbent (CCL)

The XRD analysis was carried out to determine the structure of the prepared activated carbon. The absence of a sharp peak reveals a predominantly amorphous structure for CCL, which present an important property for an excellent biosorbent **[37]**. As presented in figure 5, the intensity of the diffraction peaks mainly observed in the range 2θ = 20-80° is 20.8673°, 26.6418°, 27.4364°, 29.4410°, 31.5664°, 39.4772°, 45.3652°, 47.5004°, 48.5601°, 59.8923°, and 83.8580°, which confirm the presence of two compounds :calcite ($CaCO_3$) and silicate (SiO_2).

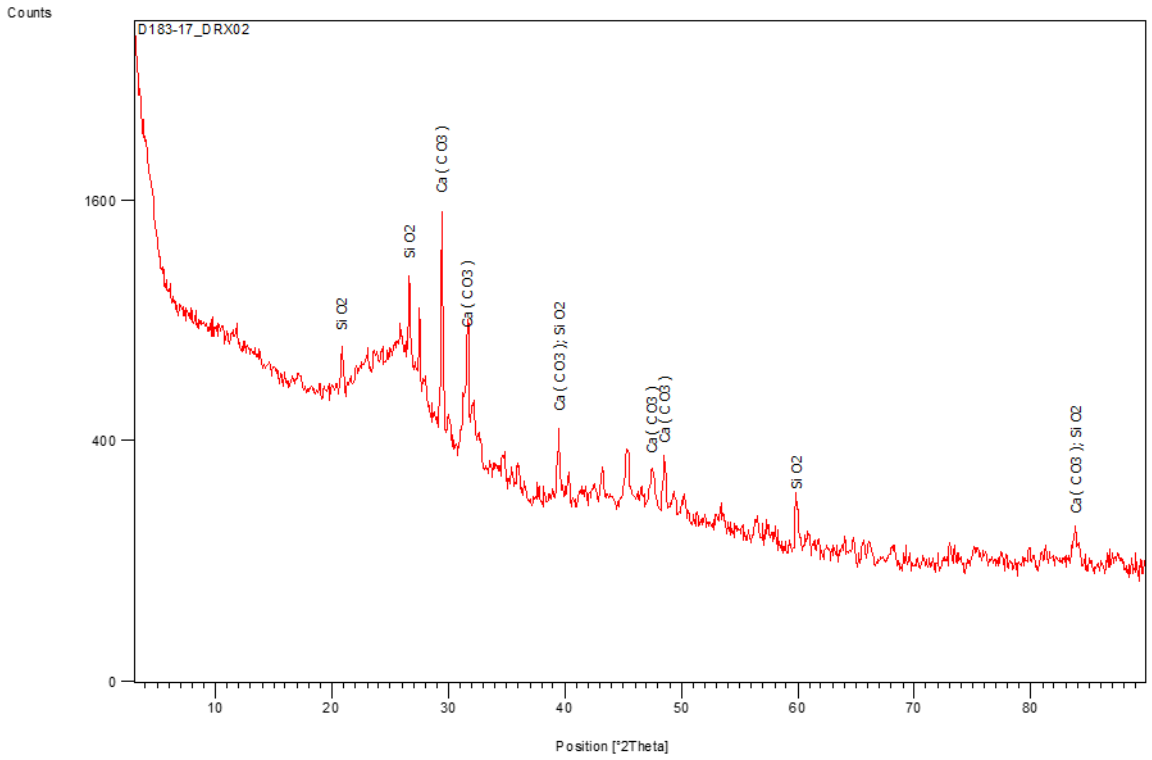

Figure 5: Powder XRD Pattern of the CCL biosorbent.

Scanning electron microscopy was performed to measure the morphological features of the CCL biosorbent. From the obtained SEM micrographs, the change in surface texture and pore development is clearly visible, whereas the biosorbent has a large distribution of grains of different sizes. As shown by figure 6, the pores available on the surface of the CCL biosorbent

289 are visible, well pronounced with distinct and smooth pore walls, due to grinding and several
290 times washing with distilled water. However, the structure looks like amorphous silica after
291 carbonization, which is a highly reactive species and can form surface complexes with the
292 cations under investigation.

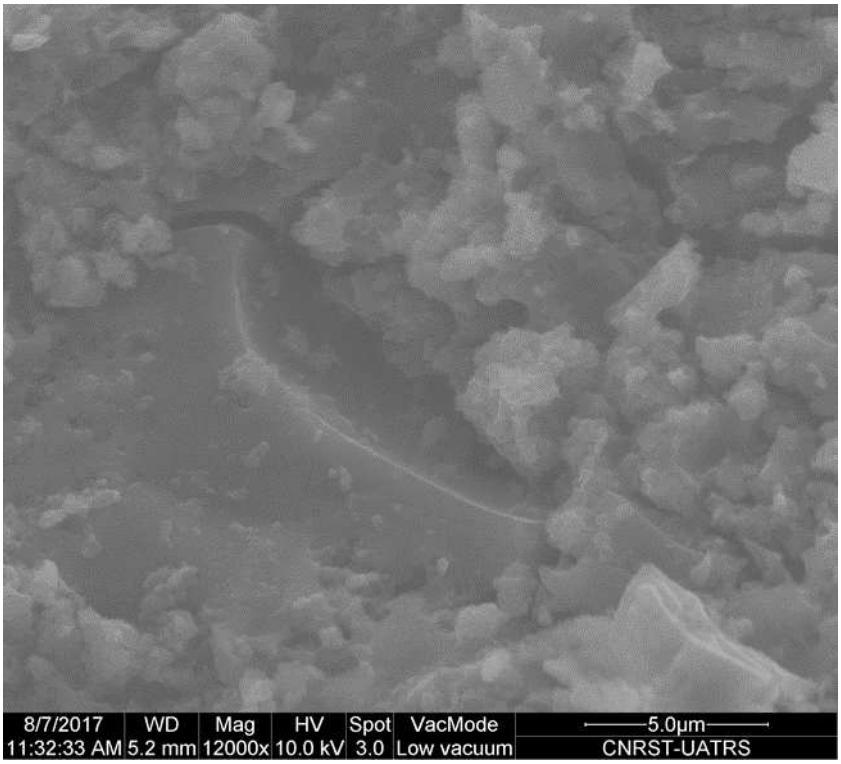

293

294 **Figure 6:** SEM micrograph of CCL biosorbent.

295 The specific surface area of CCL was determined by Brunauer-Emmett-Teller (BET)
296 multipoint technique by adsorption-desorption isotherms of nitrogen at its liquid temperature
297 (77K) and was found S_p = 15 m^2/g. The specific surface area (BET) is outstanding by
298 comparing it with that of other biosorbents derived from a natural origin.

299 **Conclusion**

300 In this work, the prime objective is the valorization of the slaughterhouse wastes and the use
301 of those raw natural materials for the preparation of low cost biosorbents with good textural
302 and structural properties. Therefore, it was crucial for this study to identify informations
303 concerning the steps of adsorbent preparation, the textural and structural characteristics of the

prepared biosorbent as well as those relating to their adsorption capacities of various inorganic pollutants. For this purpose, the biosorbent was prepared from calcined cow leather (CCL) and have been used successfully as an adsorbing agent for the removal of active pharmaceutical ingredient (Sodium Diclofenac) from aqueous solutions. After activation, we carried out characterization tests by physico-chemical methods (FX, DRX, IRTF and SEM) and we found that CCL is essentially composed of oxygen and carbon which gives it a structure of calcite ($CaCO_3$) and silicate (SiO_2). With the increase of concentration from 10mg/L to 50mg/L, the removal efficiency increases from 68.57% to 87.71% for diclofenac sodium (SD) reaching the equilibrium at 20mg/L. The kinetic model fits the experimental data of the pseudo-second-order better than the pseudo-first-order model, as it correlates the experimental data well for all concentrations for the anti-inflammatory under investigation. Modelling of equilibrium isotherms according to the linear and non-linear models of Langmuir, Freundlich, Temkin, Elovich and D-R was performed. Based on the R^2 coefficient values, the analysis of non-linear and linear forms for SD shows that the non-linear form of Langmuir model has a better R^2 correlation coefficient, while the linear model of Temkin has a high R^2 correlation coefficient for the adsorption of SD. The analysis of the error function results confirms the model determined based on the R^2 correlation coefficient values for the nonlinear regression, but disagrees with the model determined by the linear regression, which confirms that the nonlinear regression is more accurate and gives exact results than the linear regression for the modeling of the adsorption isotherms.

Acknowledgements

We are thankful to University Hassan II, University of Orleans, National Laboratory of drugs control Rabat, Cadi Ayyad University and Sultan Moulay Slimane University for providing necessary facilities for research work.

Availability of data and materials

The data used to support the findings of this study are available from the corresponding author upon request.

Competing interests

The authors declare they have no competing interests.

Funding

This research received no specific grant from any funding agency in the public, commercial, or not-for-profit sectors.

Authors' contributions

H. HIYANE: Writing - original draft, Software, Investigation. **S. BENKADDOUR:** Investigation. **R. SLIMANI:** Writing - review & editing. **B. CAGNON:** review & editing, Supervision. **K. KARROUCHI:** review & editing, Supervision. **M. EL HADDAD:** Writing - review & editing. **Y.ACHOUR:** Writing - review & editing, Supervision. **S. EL ANTRI:** Writing - review & editing, Supervision. **S. LAZAR:** Writing - review & editing, Supervision.

References

[1] Ali AM, Sydnes LK, Alarif WM, Al-Lihaibi SS, Aly MM, Aanrud SG, Kallenborn R. Diclofenac and two of its photooxidation products in the marine environment: Their toxicology and occurrence in Red Sea coastal waters. J Environ Chem Ecotoxicol. 2019; 1: 19-25.

[2] Jodeh S, Abdelwahab F, Jaradat N, Warad I, Jodeh W. Adsorption of diclofenac from aqueous solution using Cyclamen persicum tubers based activated carbon (CTAC). J Assoc Arab Univ Basic Appl Sci. 2016; 20: 32-38.

[3] De Luna MDG, Murniati, Budianta W, Rivera KKP, Arazo RO. Removal of sodium diclofenac from aqueous solution by adsorbents derived from cocoa pod husks. J Environ Chem Eng. 2017; 5(2): 1465-1474.

[4] Larous S, Meniai AH. Adsorption of Diclofenac from aqueous solution using activated carbon prepared from olive stones. Int J Hydrog Energy. 2016; 41(24): 10380-10390.

[5] Malhotra M, Suresh S, Garg A. Tea waste derived activated carbon for the adsorption of sodium diclofenac from wastewater: adsorbent characteristics, adsorption isotherms, kinetics, and thermodynamics. Environ Sci Pollut Res. 2018; 25: 32210–32220.

[6] Saucier C, Adebayo MA, Lima EC, Cataluña R, Thue PS, Prola LDT, Puchana-Rosero MJ, Fernando MM, Pavan FA, Dotto GL. Microwave-assisted activated carbon from cocoa shell as adsorbent for removal of sodium diclofenac and nimesulide from aqueous effluents. J Hazard Mater. 2015; 289: 18-27.

[7] Bernardo M, Rodrigues S, Lapa N, Matos I, Lemos F, Batista MKS, Fonseca I. High efficacy on diclofenac removal by activated carbon produced from potato peel waste. Int J Environ Sci Technol. 2016; 13: 1989–2000.

[8] García-Sabido D, López-Mesas M, Carrillo- Navarrete F. Chicken feather fibers waste as a low-cost biosorbent of acid blue 80 dye. Desalin Water Treat. 2016; 57(8): 3732-3740.

[9] Slimani R, Anouzla A, Abrouki Y, Ramli Y, El Antri S, Mamouni R, Lazar S, El Haddad M. Removal of a cationic dye -Methylene Blue- from aqueous media by the use of animal bone meal as a new low cost adsorbent. J Mater Environ Sci. 2011; 2: 77-87.

[10] Hachoumi I, El Ouahabi I, Slimani R, Cagnon B, El Haddad M, El Antri S, Lazar S. Adsorption studies with a new biosorbent Ensis siliqua shell powder for removal two textile dyes from aqueous solution. J Mater Environ Sci. 2017; 8: 1448-1459.

[11] Hossain A, Aditya G. Cadmium biosorption potential of shell dust of the freshwater invasive snail *Physa acuta*, J Environ Chem Eng. 2013; 1(3): 574-580.

375 [12] National Center for Biotechnology Information. PubChem Database. Diclofenac sodium.
376 2020.

377 [13] Matin AA, Farajzadeh MA, Jouyban A. A simple spectrophotometric method for
378 determination of sodium diclofenac in pharmaceutical formulations. Farmaco. 2005; 60(10):
379 855–858.

380 [14] Mona S, Kaushik A, Kaushik CP. Biosorption of reactive dye by waste biomass of *Nostoc*
381 *linckia*, J Ecol Eng. 2011; 37(10): 1589–1594.

382 [15] Langmuir I. The adsorption of gases on plane surfaces of glass, mica and platinum. JACS.
383 1918; 40: 1361-1403.

384 [16] Freundlich H. Colloid and Capillary Chemistry. Methuen, London. 1926; 114-122.

385 [17] Freundlich H. Kapillarchemie. Akademische Verlagsgesellschaft ,Leipzig, Germany.
386 1909.

387 [18] Tempkin MJ, Pyzhev V. Kinetics of ammonia synthesis on promoted iron catalysts. Acta
388 Physicochim URSS. 1940; 12: 217-256.

389 [19] Elovich SY, Larinov OG. Theory of adsorption from solutions of non electrolytes on solid
390 (I) equation adsorption from solutions and the analysis of its simplest form, (II) verification of
391 the equation of adsorption isotherm from solutions. Izv Akad Nauk SSSR Otd Khim Nauk.
392 1962; 2: 209-216.

393 [20] Dubinin MM. The potential theory of adsorption of gases and vapors for adsorbents with
394 energetically non-uniform surface. Chem Rev. 1960; 60: 235–266.

395 [21] Ho YS, McKay G. Sorption of dye from aqueous solution by peat. Chem Eng J. 1998; 70:
396 115-124.

[22] Bhattacharyya KG, Sharma A. Kinetics and thermodynamics of Methylene Blue adsorption on Neem (*Azadirachta indica*) leaf powder. Dyes Pigm. 2005; 65: 51-59.

[23] Kumar KV, Porkodi K, Rocha F. Isotherms and thermodynamics by linear and nonlinear regression analysis for the sorption of methylene blue onto activated carbon: Comparison of various error functions. J Hazard Mater. 2008; 151(2-3): 794-804.

[24] Gimbert F, Morin-Crini N, Renault F, Badot PM, Crini G. Adsorption isotherm models for dye removal by cationized starch-based material in a single component system: Error analysis. J Hazard Mater. 2008; 157(1): 34-46.

[25] Chan LS, Cheung WH, Allen SJ, McKay G. Error Analysis of Adsorption Isotherm Models for Acid Dyes onto Bamboo Derived Activated Carbon. Chin J Chem Eng. 2012; 20: 535-542.

[26] Porter JF, McKay G, Choy KH. The prediction of sorption from a binary mixture of acidic dyes using single- and mixed-isotherm variants of the ideal adsorbed solute theory. Chem Eng Sci. 1999; 54: 5863–5885.

[27] Marquardt DW. An algorithm for least squares estimation of non-linear parameters. J Soc Ind Appl Math. 1963; 11: 431–441.

[28] Kapoor A, Yang RT. Correlation of equilibrium adsorption data of condensable vapours on porous adsorbents. Gas Sep Purif. 1989; 3: 187–192.

[29] Mall ID, Srivastava V, Agarwal N. Removal of Orange-G and Methyl Violet dyes by adsorption onto bagasse fly ash-kinetic study and equilibrium isotherm analyses. Dyes Pigm. 2006; 69: 210-223.

418 [30] E. Demirbas, M. Kobya, A.E.S. Konukman. Error analysis of equilibrium studies for the
419 almond shell activated carbon adsorption of Cr(VI) from aqueous solutions. J Hazard Mater.
420 2008; 154: 787-794.

421 [31] Gunay A. Application of nonlinear regression analysis for ammonium exchange by natural
422 (Bigadic) clinoptilolite. J Hazard Mater. 2007; 148: 708-713.

423 [32] Tseng RL, Tseng SK. Pore structure and adsorption performance of the KOH-activated
424 carbons prepared from corncob. J Colloid Interface Sci. 2005; 287: 428-437.

425 [33] Achour Y, Bahsis L, Ablouh EH, Yazid H, Laamari MY, El Haddad M. Insight into
426 Adsorption mechanism of Congo red dye onto Bombax Buonopozense bark Activated-carbon
427 using Central composite design and DFT studies. Surf Interfaces. 2021; 23: 100977.

428 [34] Achour Y, El Kassimi A, Nadir I, Yazid H, Hafid A, Khouili M, El Himri M, Laamari
429 MY, El Haddad M. Simultaneous Removal of Binary Mixture of Cationic Dyes onto Bombax
430 Buonopozense Bark: Plackett–Burman and Central Composite Design. 2022; 12(1): 326-338.

431 [35] Guo J, Lua AC. Textural and chemical properties of adsorbent prepared from palm shell
432 by phosphoric acid activation. Mater Chem Phys. 2003; 80: 114-119.

433 [36] Jung MW, Ahn KH, Lee Y, Kim KP, Rhee JS, Tae PJ, Paeng KJ. Adsorption characteristic
434 of phenol and chlorophenols on granular activated carbons (GAC). Microchem J. 2001; 70:
435 123-131.

436 [37] Madhava RM, Reddy DHKK, Venkateswarlu P, Seshaiah K. Removal of mercury from
437 aqueous solutions using activated carbon prepared from agricultural by product/waste. J
438 Environ Manage. 2009; 90: 634-643.

Figures

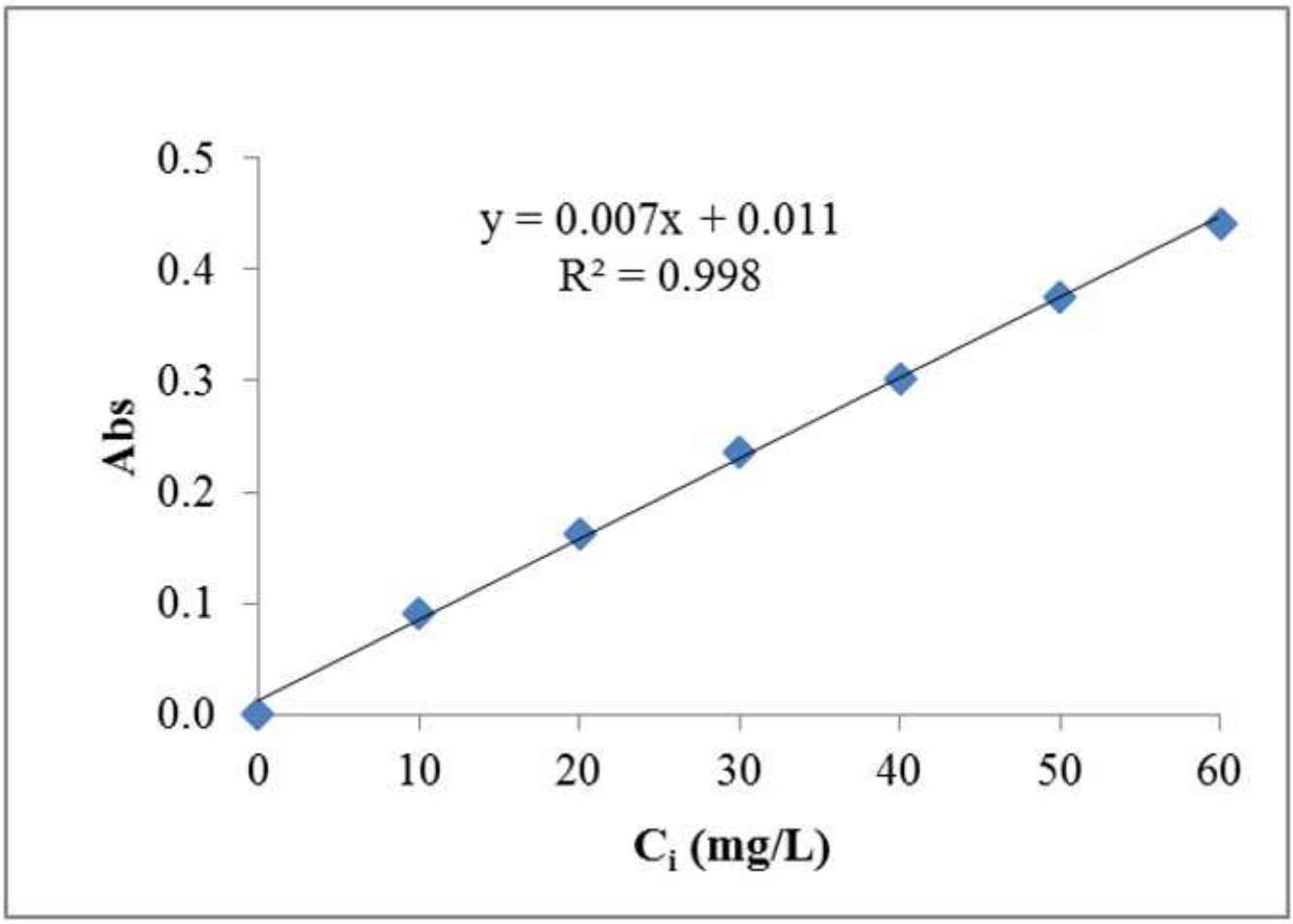

Figure 1

Calibration curve of SD.

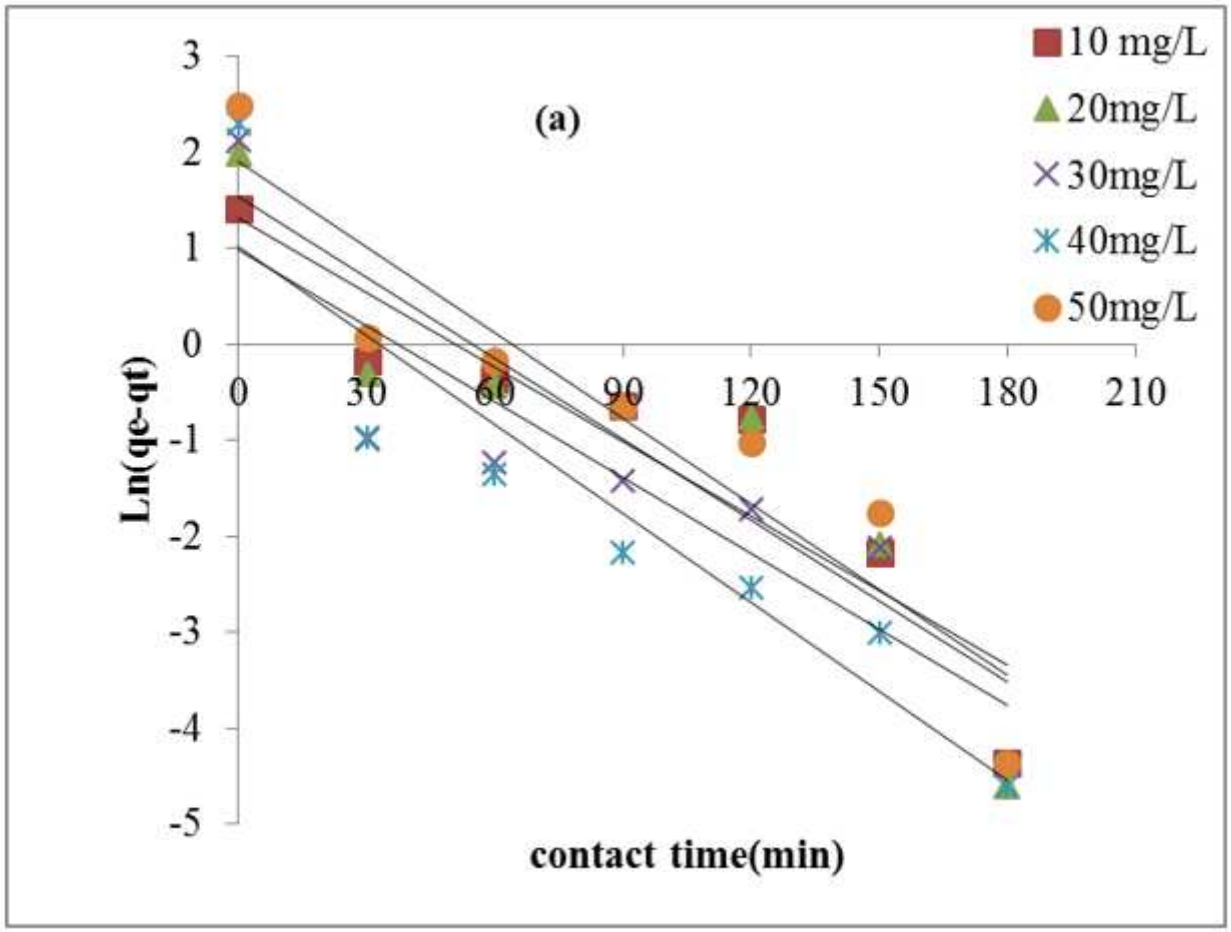

Figure 2

Linearized plots for Pseudo-first-order kinetics for biosorption of sodium diclofenac (SD) onto CCL biosorbent.

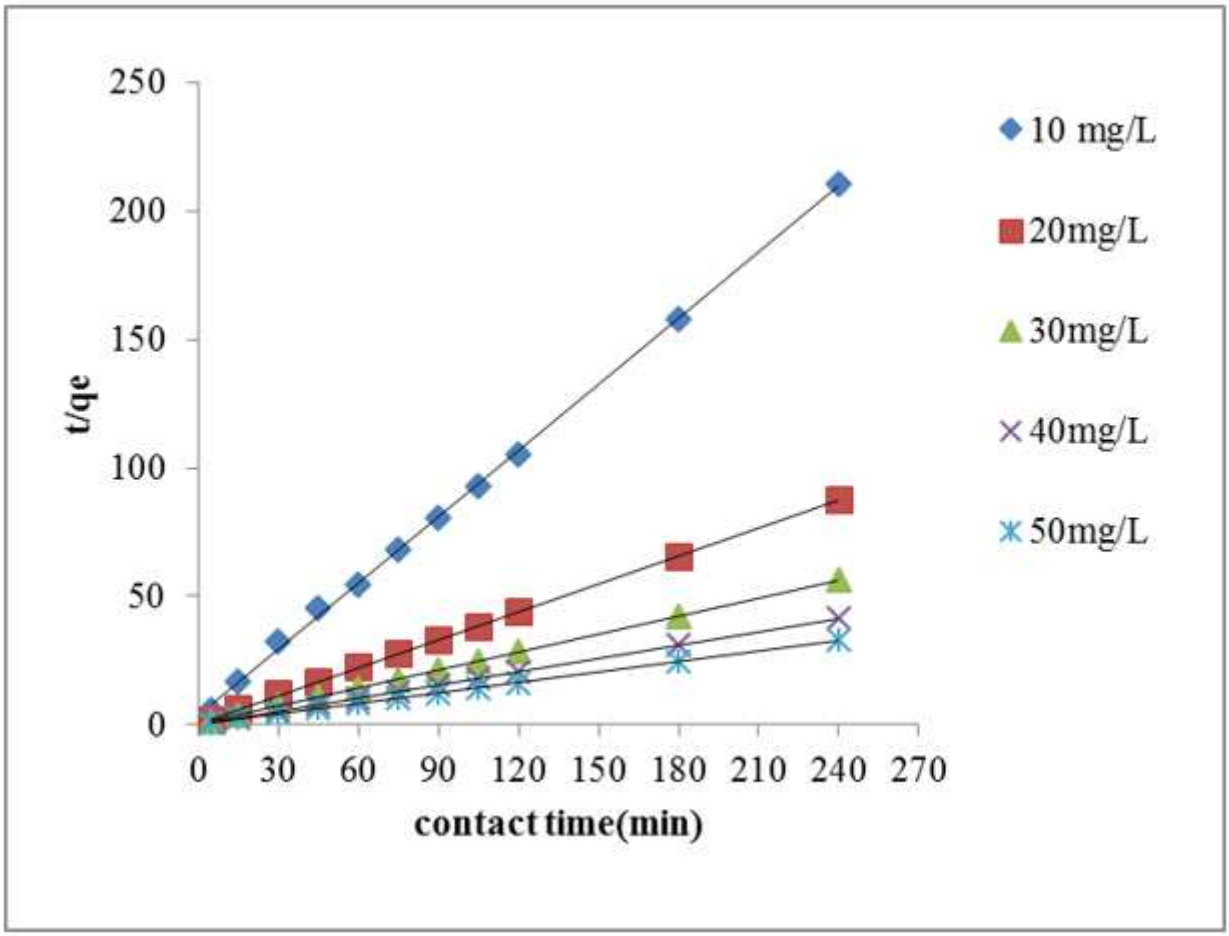

Figure 3

Linearized plots for Pseudo-second-order kinetics for biosorption of sodium diclofenac (SD) onto CCL biosorbent.

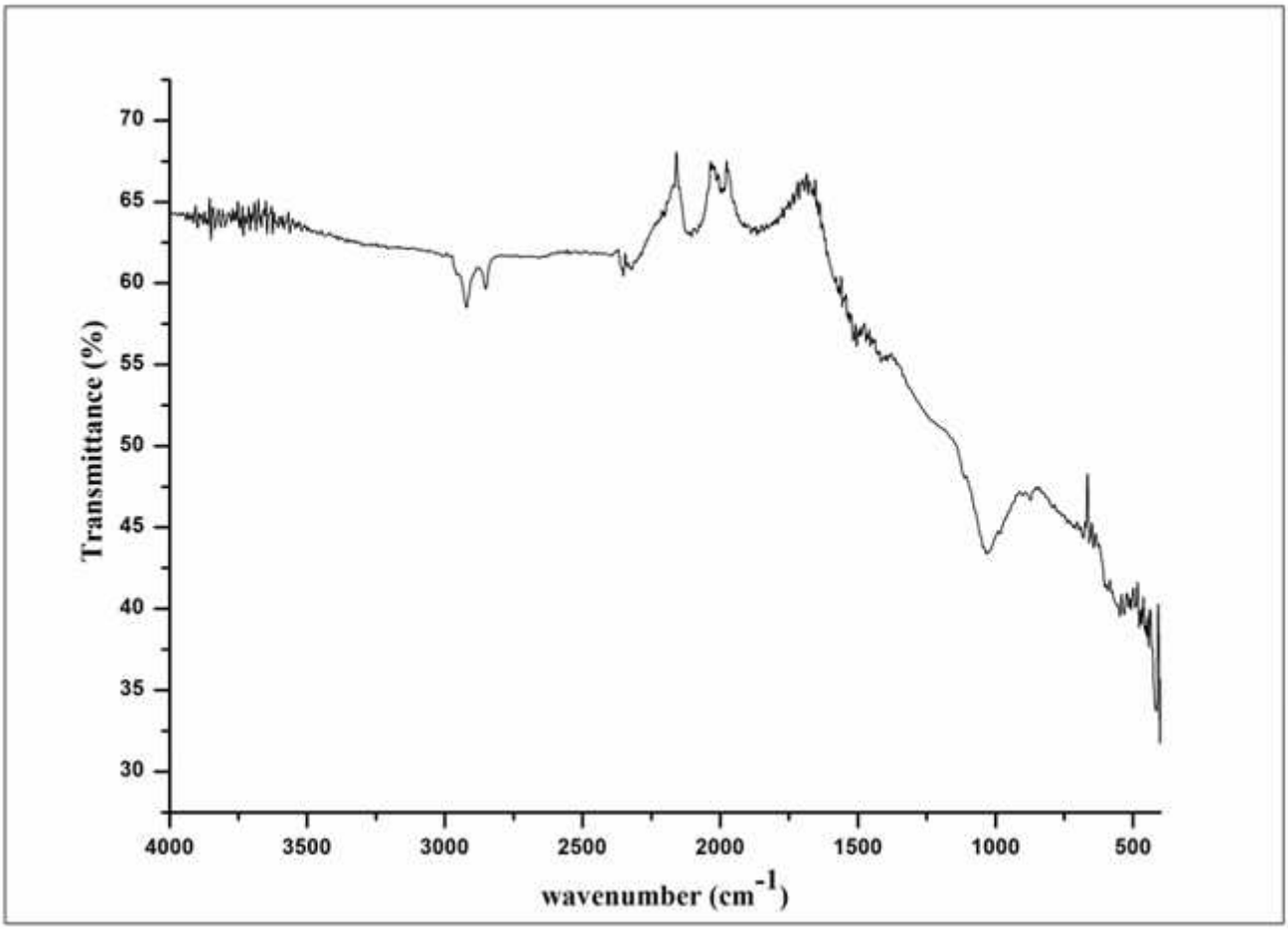

Figure 4

IR spectrum of biosorbent (CCL)

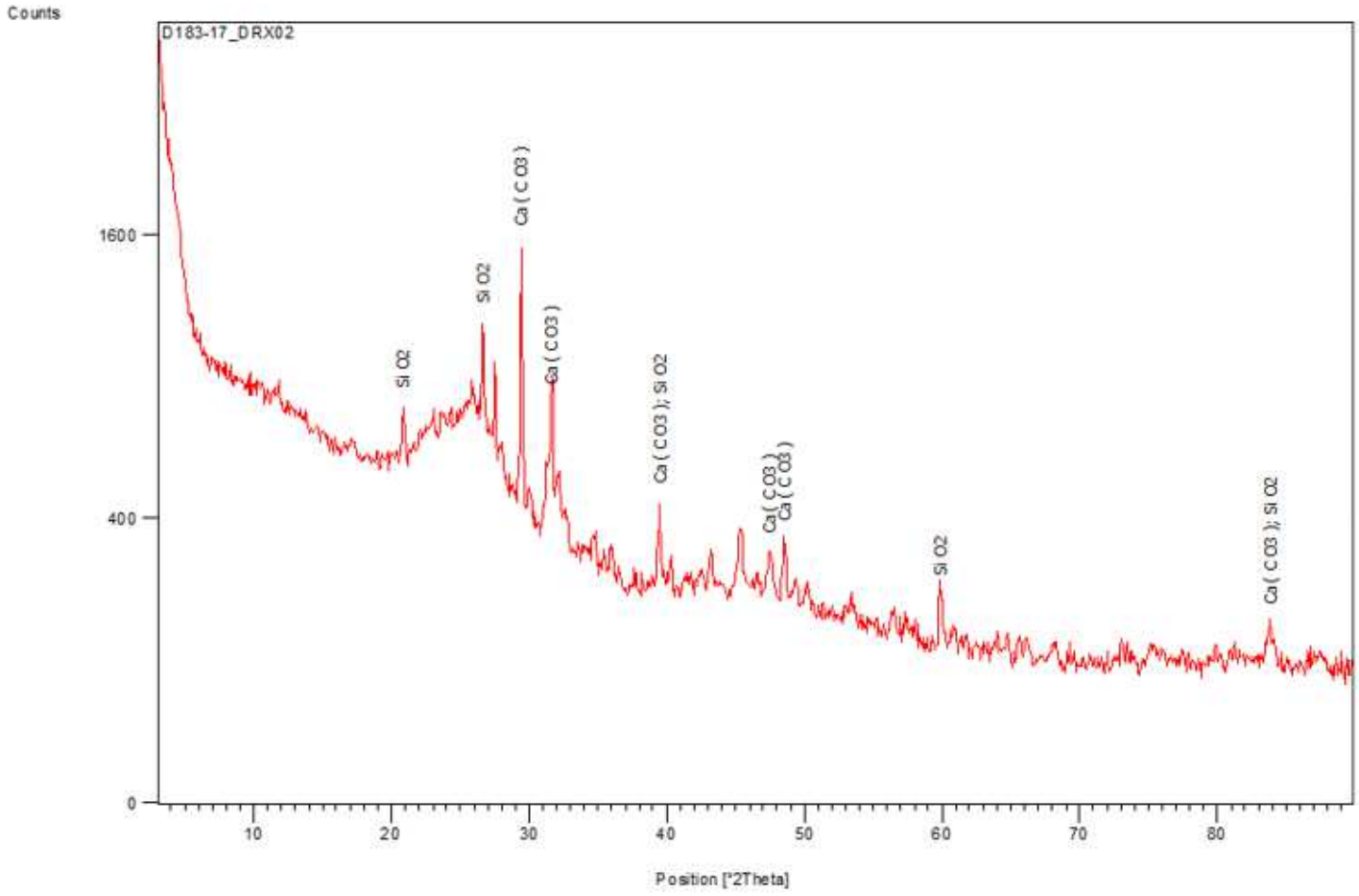

Figure 5

Powder XRD Pattern of the CCL biosorbent.

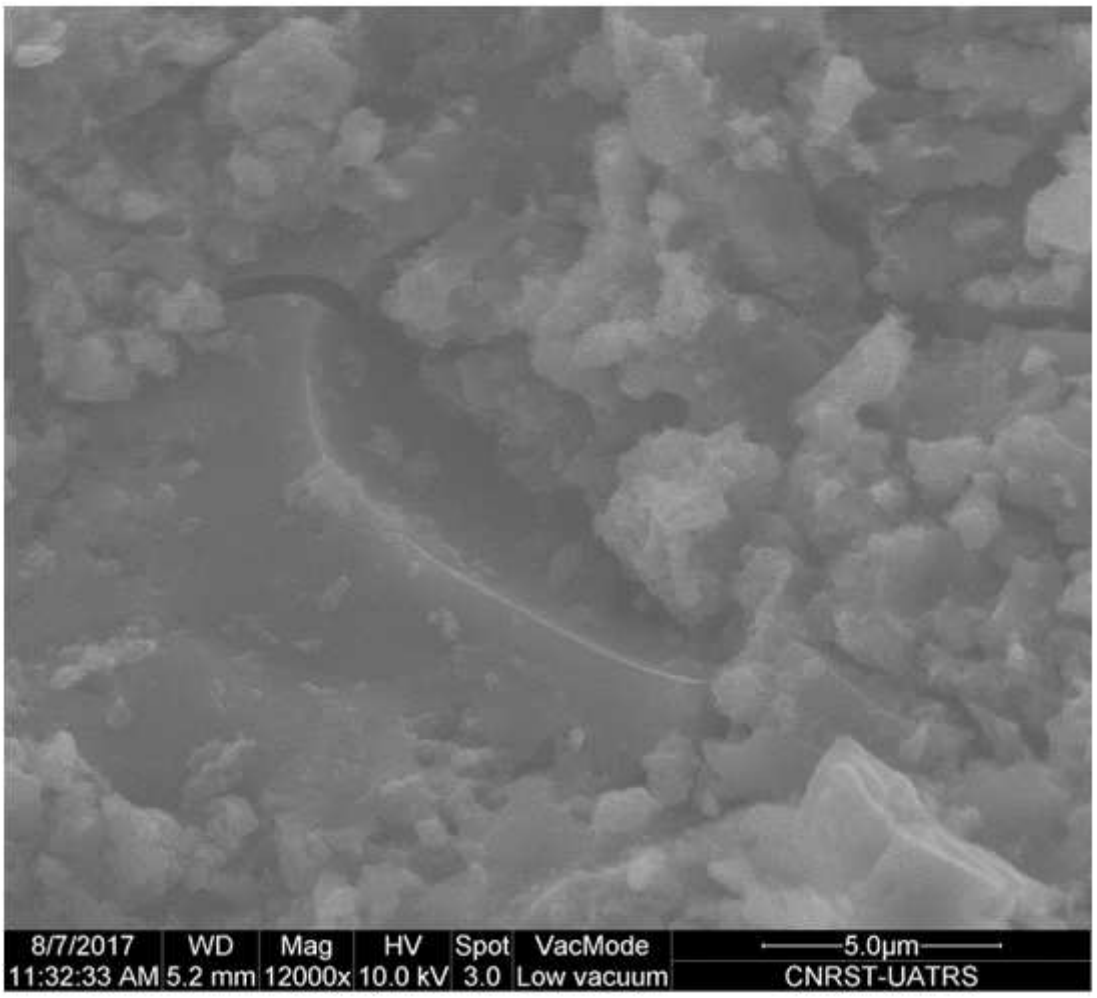

Figure 6

SEM micrograph of CCL biosorbent.